

# Multi-pass oscillator layout for high-energy mode-locked thin-disk lasers

K. Schuhmann<sup>1,2,\*</sup>, K. Kirch<sup>1,2</sup> and A. Antognini<sup>1,2</sup>

<sup>1</sup> Institute for Particle Physics, ETH, 8093 Zurich, Switzerland

<sup>2</sup> Paul Scherrer Institute, 5232 Villigen-PSI, Switzerland

\* [skarsten@phys.ethz.ch](mailto:skarsten@phys.ethz.ch)

## Abstract:

A novel optical layout for a multi-pass resonator is presented paving the way for pulse energy scaling of mode-locked thin-disk lasers. The multi-pass resonator we are proposing consists of a concatenation of nearly identical optical segments. Each segment corresponds to a round-trip in an optically stable cavity containing an active medium exhibiting soft aperture effects. This scheme is apt for energy and power scaling because the stability region of this multi-pass resonator contrarily to the 4f-based schemes does not shrink with the number of passes. Simulation of the eigen-mode of this multi-segment resonator requires considering aperture effects. This has been achieved by implementing effective Gaussian apertures into the ABCD-matrix formalism as lenses with imaginary focal length. We conclude proposing a simple way to double the stability region of the state-of-the-art layouts used in industry achievable by a minimal rearrangement of the used optical components.

© 2016 Optical Society of America

**OCIS codes:** (140.3410) Laser resonators, (140.3615) Lasers, ytterbium, (140.4050) Mode-locked lasers, (140.4780) Optical resonators, (140.6810) Thermal effects, (140.7090) Ultrafast lasers

---

## References and links

1. U. Keller, "Ultrafast solid-state laser oscillators: a success story for the last 20 years with no end in sight," *Applied Physics B* **100**, 15–28 (2010).
2. F. Krausz and M. Ivanov, "Attosecond physics," *Rev. Mod. Phys.* **81**, 163–234 (2009).
3. T. Südmeyer, S. V. Marchese, S. Hashimoto, C. R. E. Baer, G. Gingras, B. Witzel, and U. Keller, "Femtosecond laser oscillators for high-field science," *Nat. Photon.* **2**, 599–604 (2008).
4. A. Giesen, H. Hügel, A. Voss, K. Wittig, U. Brauch, and H. Opower, "Scalable concept for diode-pumped high-power solid-state lasers," *Applied Physics B* **58**, 365–372 (1994).
5. A. Giesen, J. Speiser, R. Peters, C. Kränkel, and K. Petermann, "Thin-disk lasers come of age", *Photonics Spectra* **41**, 52–58 (2007).
6. <http://www.trumpf.com>
7. T. Gottwald, C. Stolzenburg, D. Bauer, J. Kleinbauer, V. Kuhn, T. Metzger, S. Schad, D. Sutter, and A. Killi, "Recent disk laser development at TRUMPF," *Proc. SPIE 8547, High-Power Lasers 2012: Technology and Systems*, 85470C (2012).
8. S. Piehler, B. Weichelt, A. Voss, M. Abdou Ahmed and T. Graf, "Power scaling of fundamental-mode thin-disk lasers using intracavity deformable mirrors", *Opt. Lett.* **37**, 5033–5035 (2012).
9. J. Mende, E. Schmid, J. Speiser, G. Spindler and A. Giesen, "Thin disk laser: power scaling to the kW regime in fundamental mode operation", *Proc. SPIE 7193, Solid State Lasers XVIII: Technology and Devices*, 71931V (2009).
10. H. Fattahi, H.G. Barros, M. Gorjan et al., "Third-generation femtosecond technology", *Optica* **1**, 45–63 (2014).
11. M. Larionov and J. Neuhaus "Regenerative thin disk amplifier with a pulse energy of 120 mJ at 1 kHz", *Advanced Solid State Lasers*, ATH2A.51 (2014).

12. C. Saraceno, F. Emaury, C. Schriber, A. Diebold, M. Hoffmann, M. Golling, T. Südmeyer, and U. Keller, "Toward millijoule-level high-power ultrafast thin-disk oscillators," *Selected Topics in Quantum Electronics, IEEE Journal of* **21**, 106–123 (2015).
13. J. Brons, V. Pervak, E. Fedulova, D. Bauer, D. Sutter, V. Kalashnikov, A. Apolonskiy, O. Pronin, and F. Krausz, "Energy scaling of Kerr-lens mode-locked thin-disk oscillators," *Opt. Lett.* **39**, 6442–6445 (2014).
14. J. Tümmler, R. Jung, H. Stiel, P. V. Nickles, and W. Sandner, "High-repetition-rate chirped-pulse-amplification thin-disk laser system with joule-level pulse energy," *Opt. Lett.* **34**, 1378–1380 (2009).
15. J. Negel, A. Loescher, A. Voss, D. Bauer, D. Sutter, A. Killi, M. Abdou Ahmed and T. Graf, "Ultrafast thin-disk multipass laser amplifier delivering 1.4 kW (4.7 mJ, 1030 nm) average power converted to 820 W at 515 nm and 234 W at 343 nm," *Opt. Express* **23**, 21064–21077 (2015)
16. N. Kanda, A. A. Eilanlou, T. Imahoko, T. Sumiyoshi, Y. Nabekawa, M. Kuwata-Gonokami, and K. Midorikawa, High-pulse-energy Yb:Yag thin disk mode-locked oscillator for intra-cavity high harmonic generation, *Advanced Solid-State Lasers Congress, AF3A.8* (2013).
17. O. Pronin, J. Brons, C. Grasse, V. Pervak, G. Boehm, M.-C. Amann, A. Apolonski, V. L. Kalashnikov, and F. Krausz, "High-power Kerr-lens mode-locked Yb:YAG thin-disk oscillator in the positive dispersion regime," *Opt. Lett.* **37**, 3543–3545 (2012).
18. M. Richardson and A. Zoubir, "High intensity MHz mode-locked," USA Patent US 7590156 B1 (2009).
19. C. J. Saraceno, F. Emaury, C. Schriber, M. Hoffmann, M. Golling, T. Südmeyer, and U. Keller, "Ultrafast thin-disk laser with 80  $\mu$ J pulse energy and 242 W of average power," *Opt. Lett.* **39**, 9–12 (2014).
20. D. Bauer, I. Zawischa, D. H. Sutter, A. Killi, and T. Dekorsy, "Mode-locked Yb:Yag thin-disk oscillator with 41  $\mu$ J pulse energy at 145 W average infrared power and high power frequency conversion," *Opt. Express* **20**, 9698–9704 (2012).
21. C. Hönninger, R. Paschotta, F. Morier-Genoud, M. Moser, and U. Keller, "Q-switching stability limits of continuous-wave passive mode locking," *J. Opt. Soc. Am. B* **16**, 46–56 (1999).
22. B. Dannecker, X. Délen, K. S. Wentsch, B. Weichelt, C. Hönninger, A. Voss, M. A. Ahmed, and T. Graf, "Passively mode-locked Yb:CaF<sub>2</sub> thin-disk laser," *Opt. Express* **22**, 22278–22284 (2014).
23. V. Magni, "Resonators for solid-state lasers with large-volume fundamental mode and high alignment stability," *Appl. Opt.* **25**, 107–117 (1986).
24. J. Speiser, "Thin disk laser-energy scaling", *Laser Physics* **19**, 274–280 (2009).
25. C. R. E. Baer, O. H. Heckl, C. J. Saraceno, C. Schriber, C. Kränkel, T. Südmeyer, and U. Keller, "Frontiers in passively mode-locked high-power thin disk laser oscillators," *Opt. Express* **20**, 7054–7065 (2012).
26. S. Gatz; J. Herrman, "Geometrical threshold zones and Gaussian modes in lasers with radially varying gain," *Opt. Lett.* **19**, 1696–1698 (1994).
27. L. W. Casperon, A. Yariv, "The Gaussian Mode in Optical Resonators with a Radial Gain Profile," *Appl. Phys. Lett.* **12**, 355–357 (1968).
28. V. Magni, "Perturbation theory of nonlinear resonators with an application to Kerr lens mode locking," *J. Opt. Soc. Am. B* **13**, 2498–2507 (1996).
29. L. W. Casperon, S. D. Lunnam, "Gaussian Modes in High Loss Laser Resonators," *Appl. Opt.* **14**, 1193–1199 (1975).
30. J. Herrman, "Theory of Kerr-lens mode locking: role of self-focusing and radially varying gain," *J. Opt. Soc. Am. B* **11**, 498–512 (1994).
31. H. Kogelnik, "On the Propagation of Gaussian Beams of Light Through Lenslike Media Inducing those with a Loss or Gain Variation," *Appl. Opt.* **4**, 1562–1569 (1965).
32. A. Siegman, *Lasers* (University Science Books, 1986).
33. D. V. Willetts, M. R. Harris, "Output Characteristics of a Compact 1 J Carbon Dioxide Laser with a Gaussian Reflectivity Resonator," *IEEE Journal of quantum electronics* **24**, 849–855 (1988).
34. A. Antognini, K. Schuhmann, F. Amaro, F. Biraben, A. Dax, A. Giesen, T. Graf, T. Hänsch, P. Indelicato, L. Julien, C.-Y. Kao, P. Knowles, F. Kottmann, E. Le Bigot, Y.-W. Liu, L. Ludhova, N. Moschuring, F. Mulhauser, T. Nebel, F. Nez, P. Rabinowitz, C. Schwob, D. Taqqu, and R. Pohl, "Thin-disk Yb:Yag oscillator-amplifier laser, ASE, and effective Yb:Yag lifetime," *IEEE Journal of Quantum Electronics* **45**, 993–1005 (2009).
35. K. Schuhmann, M. A. Ahmed, A. Antognini, T. Graf, T. W. Hänsch, K. Kirch, F. Kottmann, R. Pohl, D. Taqqu, A. Voss, and B. Weichelt, "Thin-disk laser multi-pass amplifier," *Proc. SPIE 9342, Solid State Lasers XXIV: Technology and Devices*, 93420U (2015).
36. R. Pohl, A. Antognini, F. Nez, F. D. Amaro, F. Biraben, J. M. R. Cardoso, D. S. Covita, A. Dax, S. Dhawan, L. M. P. Fernandes, A. Giesen, T. Graf, T. W. Hänsch, P. Indelicato, L. Julien, C.-Y. Kao, P. Knowles, E.-O. Le Bigot, Y.-W. Liu, J. A. M. Lopes, L. Ludhova, C. M. B. Monteiro, F. Mulhauser, T. Nebel, P. Rabinowitz, J. M. F. dos Santos, L. A. Schaller, K. Schuhmann, C. Schwob, D. Taqqu, J. F. C. A. Veloso, and F. Kottmann, "The size of the proton," *Nature* **466**, 213–216 (2010).
37. A. Antognini, F. Nez, K. Schuhmann, F. D. Amaro, F. Biraben, J. M. R. Cardoso, D. S. Covita, A. Dax, S. Dhawan, M. Diepold, L. M. P. Fernandes, A. Giesen, A. L. Gouvea, T. Graf, T. W. Hänsch, P. Indelicato, L. Julien, C.-Y. Kao, P. Knowles, F. Kottmann, E.-O. Le Bigot, Y.-W. Liu, J. A. M. Lopes, L. Ludhova, C. M. B. Monteiro, F. Mulhauser, T. Nebel, P. Rabinowitz, J. M. F. dos Santos, L. A. Schaller, C. Schwob, D. Taqqu, J. F.

- C. A. Veloso, J. Vogelsang, and R. Pohl, “Proton structure from the measurement of 2s-2p transition frequencies of muonic hydrogen,” *Science* **339**, 417–420 (2013).
38. M. Kumkar, “Laser amplifying system”, Germany Patent DE 10140254 A1 (2003).
39. P. B. Lundquist, S. Sarkisyan, E. A. Wilson, R. M. Copenhaver, H. Martin and S. McCahon, “Off axis walk off multi-pass amplifiers”, US Patent US 8605355 (2013).
40. K. Schuhmann, T. W. Hänsch, K. Kirch, A. Knecht, F. Kottmann, F. Nez, R. Pohl, D. Taquu and A. Antognini, “Thin-disk laser pump schemes for large number of passes and moderate pump source quality,” *Appl. Opt.* **54**, 9400-9408 (2015).

## 1. Motivation

Ultra-short laser pulse sources [1, 2] enable a large variety of fundamental physics investigations, as well as technological and industrial applications. Many applications in industry and strong-field physics will tremendously benefit from the increase of the pulse energy in the mJ regime at few MHz repetition rates [3]: on one hand production throughput and material compendium extension especially for materials where non-linear multi-photon absorption is required, and on the other hand, reduced measurement times, increased signal to noise, and new scientific possibilities.

Mode-locked thin-disk [4, 5] lasers are widely used in research laboratories and in industry because of their power scaling and high pulse energy capabilities [6, 7, 8, 9, 10, 11, 12, 13, 14, 15, 16, 17]. The output pulse energy  $E$  of a mode-locked thin-disk laser can be increased, at a given average output power  $P_{\text{avg}}$ , by reducing the laser repetition rate  $f_{\text{rep}}$ , given the simple relation  $E = P_{\text{avg}}/f_{\text{rep}}$  from energy conservation. Smaller repetition rates can be achieved simply by increasing the oscillator cavity length. One successful way to increment the resonator length was obtained by inserting into the cavity a Herriott cell [18, 19]. However, the elevated intra-cavity pulse energy achieved in this way required operation of the oscillator in an evacuated environment to avoid detrimental non-linear effects in air [19].

The cavity length can be also increased by folding the laser beam on the active medium (thin-disk) several times per round-trip [7, 20]. The large gain per round-trip achievable with such an active multi-pass cell enables large output coupling, which brings along a reduction of the intra-cavity power. Hence, this scheme providing a long cavity and decreased intra-cavity intensity is twofold advantageous and is qualified for industrial applications as it allows operation in air. Another important feature of a multi-pass resonator scheme is the reduction of Q-switching instabilities due to a linear decrease of the gain saturation fluence with the number of reflections at the thin-disk [21, 22].

The multi-pass active cells realized to date [7, 20] are based on relay 4f-imaging: 4f optical segments are used to image the thin-disk from pass to pass so that the beam propagation in the active multi-pass cell proceeds following the scheme disk-4f-disk-4f-disk-4f... The 4f propagation from the optical point of view corresponds to a zero effective length propagation and it does not provide stability for misalignment or variation of the thin-disk focal strength. Hence, to realize a stable laser operation, the 4f multi-pass cell has to be embedded in a stable optical resonator [7]. The 4f multi-pass cell with  $N$  number of passes can be described as a single-pass having a total optical length of  $L_{\text{multi-pass}} = (N - 1)L$ , a gain of  $g_{\text{multi-pass}} = g^N$ , and an active medium dioptric power of  $V_{\text{multi-pass}} = NV$ , where  $L = 4f$  represents the length of a single 4f-imaging stage,  $g$  the single-pass gain, and  $V$  the thin-disk dioptric power. Due to these cumulative effects, the resonator stability zones [23] of an oscillator containing such a multi-pass 4f-based cell shrink linearly with the number of passes  $N$  as shown in Fig. 1 for variations of the disk thermal lens [24]. This shrinking limits energy and power scaling [25].

In summary, the 4f-based multi-pass oscillators show a limited energy scaling (capitalizing only on the advantages related to the long cavity length and the reduction of the intracavity circulating intensity) but suffer for the shrinking of the stability region with the number of

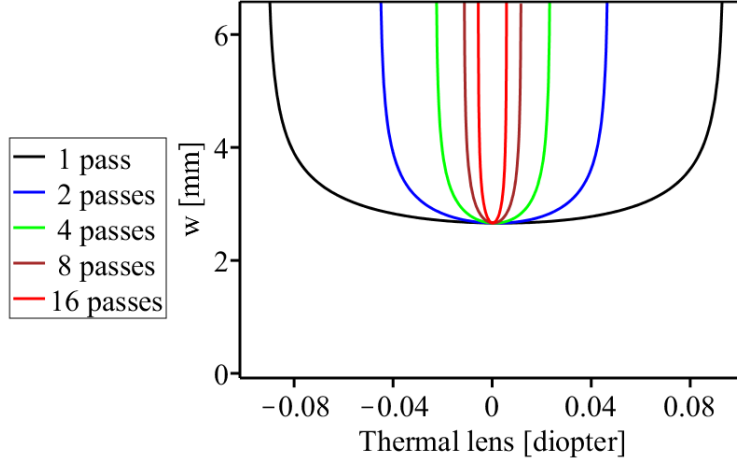


Fig. 1. (Color online) Stability plots of multi-pass resonators based on 4f-imaging stages. Plotted are the cavity eigen-mode (TEM<sub>00</sub>-mode) waist  $w$  at the thin-disk position for variations of the thin-disk thermal lens from the layout value. The shrinking of the stability region with the number of passes per cavity round-trip arising in 4f-based multi-pass resonators is demonstrated. We computed these diagrams using the ABCD-matrix formalism and by embedding the 4f-stages at the thin-disk position of the stable resonator depicted in Fig. 2 (b). A wavelength of 1030 nm was used. For a given eigen-mode size the stability plots do not depend on the specific layout of the resonator.

passes which reduces the maximal achievable output power. In this paper a novel multi-pass resonator scheme is presented which overcomes the thermal lens related power and energy limitations of state-of-the-art multi-pass mode-locked laser oscillators. In Sec. 2 our multi-pass scheme is exposed whose stability regions do not shrink with the number of passes. This opens the way for further energy and power scaling. A preliminary proof of principle of this new scheme is given in Sec. 3 while in Sec. 4 a design merging the to date 4f-based industrial scheme with our scheme is presented.

## 2. New multi-pass resonator design

The multi-pass resonator we are proposing is based on a concatenation of identical (or nearly identical) segments. Each segment corresponds to a round-trip in an optically stable resonator containing one pass (or more) on the same active medium, which exhibits soft-aperture effects.

Since the multi-pass oscillator is inheriting the eigen-mode properties of the underlying segment, we design this segment to be stable and insensitive to thermal lens variations. An example of a stable resonator whose round-trip propagation gives rise to a segment is shown in Fig. 2 (a). It is formed by a plane end-mirror M2, a thin-disk acting as concave mirror, a convex mirror (Vex) and a flat end-mirror M1. The eigen-mode waist  $w$  evolution along this cavity is shown in Fig. 2 (b). This cavity is widely used [23] because it provides an out-coupling mirror M2 with out-coupled beam waist (and divergence) insensitive to variations of the thin-disk thermal lens as demonstrated by the blue continuous curve in Fig. 2 (c) representing the eigen-mode waist at the mirror M2 position for variations of the thin-disk thermal lens. For comparison the beam waist at the other end-mirror M1 which features a larger dependency on the thermal lens variation is given as well (green dashed curve). This resonator layout is extensively used also because it allows for simple adjustments of the mode properties: the distance between thin-disk and the convex mirror can be adapted to shift the stability region of the cavity, while the beam

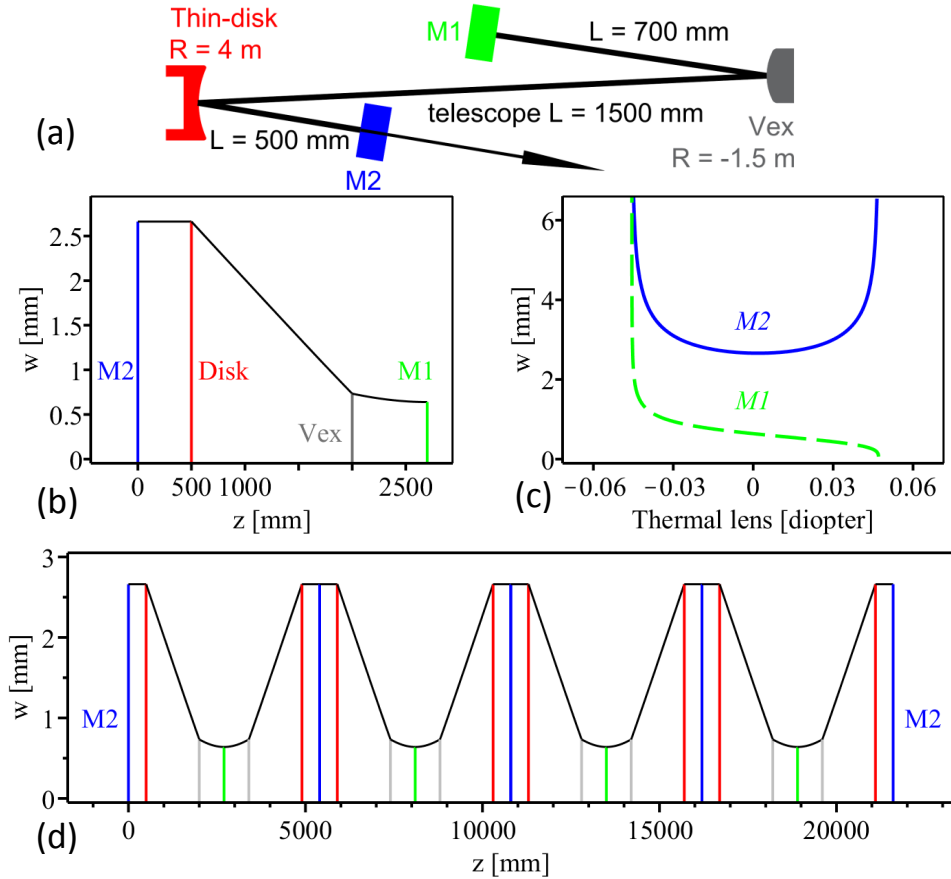


Fig. 2. (Color online) Scheme of the optical layout and properties of a multi-pass resonator as a concatenation of identical optically stable segments. (a) Standard thin-disk laser resonator layout given by a flat end-mirror  $M1$ , a convex mirror, a concave thin-disk (red) and a flat end-mirror  $M2$ . (b) Corresponding eigen-mode waist  $w$  evolution along the resonator. (c) Corresponding stability plot. Plotted is the eigen-mode waist at the  $M1$  and  $M2$  mirror positions for variations of the thin-disk thermal lens from the layout value. (d) Multi-pass resonator layout and eigen-mode waist evolution resulting by concatenating 8 times the optical segment of (a). The stability plot for the multi-segment resonator is identical to the single-segment stability plot shown in (c). The position of the optical elements are indicated by the vertical lines. The diagrams have been computed using the ABCD-matrix formalism and assuming TEM00 mode.

waist in the center of the stability region can be adjusted by adapting the distance between the  $M1$  and the convex mirrors.

As already mentioned, the multi-pass resonator according to our scheme is obtained by concatenating multiple times the same optically stable segment: each segment corresponding to a round-trip propagation in a stable cavity. An example of such a concatenation is shown in Fig. 2 (d) where 8 segments based on the cavity shown in Fig. 2 (a) enables 16 reflections at the thin-disk per round-trip. The stability regions of this multi-pass resonator coincide with the stability regions of a single segment (given in Fig. 2 (c)) provided all segments are identical. However, small differences between segments are unavoidable when practically realizing

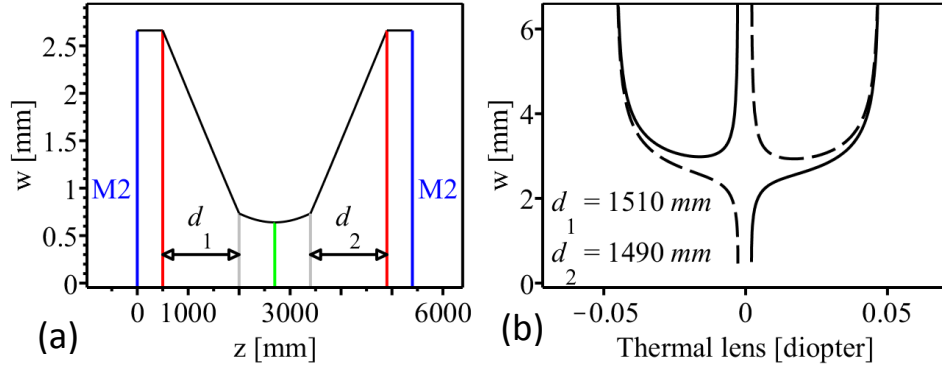


Fig. 3. (Color online) (a) Optical layout and eigen-mode waist  $w$  of a two-segment resonator with 4 reflections at the thin-disk per round-trip. (b) Corresponding stability plot. Plotted is the eigen-mode waist  $w$  at the two end-mirror positions M2 for variations of the thin-disk thermal lens from the layout value. A small asymmetry has been introduced ( $d_1 \neq d_2$ ) between the two segments which induces a discontinuity in the center of the stability region (cf. with Fig. 2 (c)).

a multi-segment oscillator because of small variations of propagation lengths, incident angles and mirror curvatures.

Consideration of this segment-to-segment asymmetries is essential for the understanding of the here proposed new multi-pass resonator concept. In fact, this design has been discarded by the thin-disk laser community because apparently these asymmetries prompt the formation of gaps in the stability region. The gap size depends on the extent of the segment-to-segment asymmetry. The formation of these gaps as a consequence of small segment-to-segment differences is exemplified in Fig. 3 for the particularly simple case that the multi-pass resonator is composed of only two segments. In the two-segment case, the gap arises in the center of the stability region. Similarly, for a multi-pass oscillator with several segments and various segment-to-segment deviations, a multitude of disruptions would apparently fragment and reduce the original stability region (of the single segment). It seems thus that the segment-to-segment asymmetries would undermine the usefulness of this scheme.

The stability plots shown in Fig. 1, 2 and 3 have been computed using the ABCD-matrix formalism. This formalism is a powerful instrument to compute eigen-mode and stability regions of resonators. However, as already noted in [26], it is mostly used for computing bare resonators neglecting the effect of the transversely varying gain in the active material. Aperture effects which naturally occur in a pumped active medium mainly due to gain (absorption) in the pumped (unpumped) regions and related diffraction (mainly outside the pumped spot) may significantly affect the eigen-mode and stability properties of the resonator [27]. These effects can be described approximatively by a Gaussian aperture at the active medium and included into the ABCD-matrix formalism as imaginary lens [29, 30, 31, 32]. The ABCD-matrix describing the thin-disk can be thus written as

$$M_{\text{thin-disk}} = \begin{bmatrix} 1 & 0 \\ -\frac{1}{f} - i\frac{\lambda}{\pi W^2} & 1 \end{bmatrix}, \quad (1)$$

where  $W$  represents the effective waist of the Gaussian aperture,  $\lambda$  the laser wavelength and  $f$  the thin-disk focal length which also includes thermal lens effects.

Standard resonator designs do not include soft aperture effects because for a single-segment resonator (see Fig. 4 (a)), the inclusion of aperture effects does not considerably alter the com-

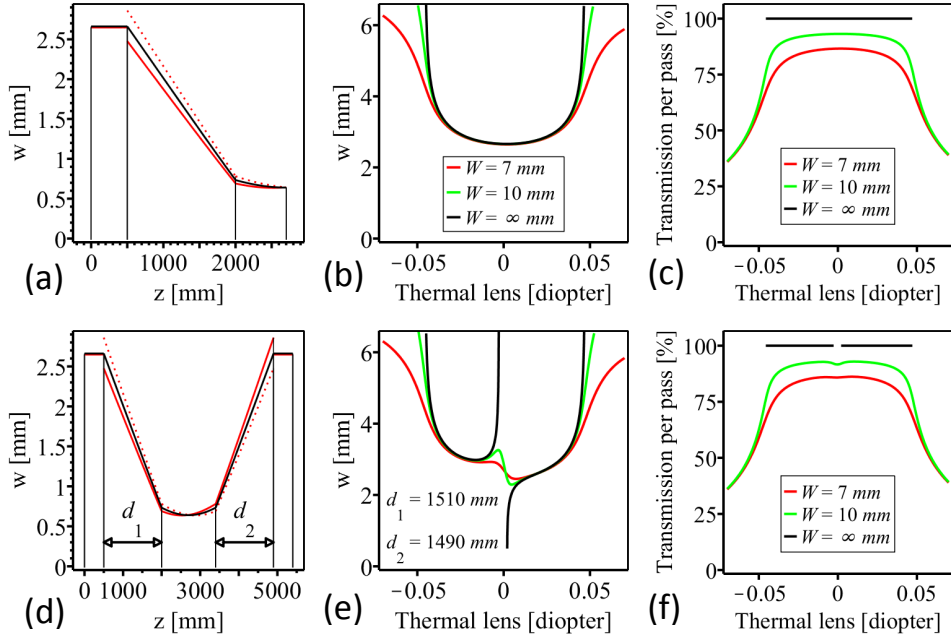


Fig. 4. (Color online) Influence of a Gaussian aperture at the active medium on the properties of a single-segment (top row) and a multi-segment (bottom row) resonators. (a) Optical layout and eigen-mode waist  $w$  evolution of a single-segment resonator. The black curve has been computed without aperture effects. The two red curves represent the back (dotted) and forth (continuous) propagation when aperture effects are included. (b) Corresponding stability plot. Plotted is the waist at the left end-mirror position for variations of the thin-disk thermal lens without aperture effects (black) and for two aperture waists  $W$  (green and red). (c) Average (over a round-trip) transmission of the eigen-mode through the Gaussian aperture for variations of the thermal lens. For an infinite sized aperture the transmission (defined only within the stability region) is 100%. (d) Similar to (a) but for a two-segment resonator. (e) Similar to (b) but for a two-segment resonator where a small asymmetry between the two segments has been introduced. The aperture effects damp the instability and close the gap in the stability region. (f) Similar to (c) for the two-segment resonator with the above specified small asymmetry. The increase of losses at the original gap position is minimal. All the curves have been computed using the ABCD-matrix formalism allowing for lenses with complex values.

puted value of the eigen-mode size for thin-disk thermal lens variations within the “original” (computed without considering the soft aperture effect) stability region (see Fig. 4 (b)). For dioptric power outside the “original” stability range, the inclusion of aperture effects results in eigen-modes with finite waist which implies an extension of the stability region [26, 33]. Therefore the inclusion of aperture effects shows that in principle laser operation may occur also outside the “original” stability region. Yet this extension has no practical relevance because outside the “original” stability range the round-trip losses caused by the aperture are increasing dramatically as demonstrated in Fig. 4 (c) and [26, 28].

Contrarily, aperture effects need to be included in the simulations of multi-segment resonators (e.g. Fig. 4 (d)) having small segment-to-segment deviations. Simulating multi-segment resonators with small segment-to-segment deviations without accounting for soft aperture effects produces wrong results because it predicts the formation of gaps within the stability region

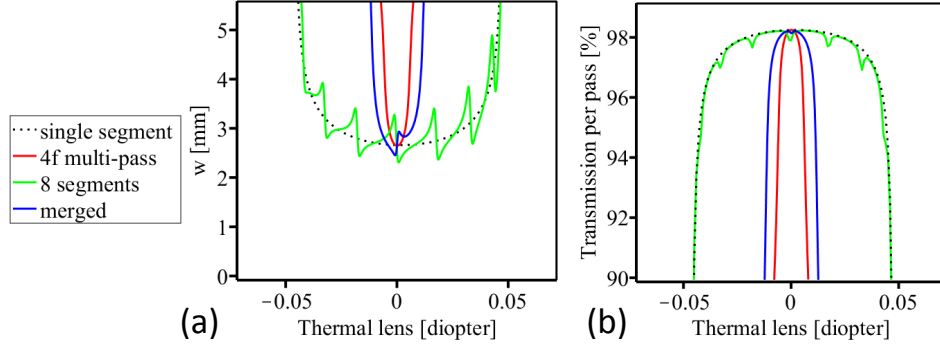


Fig. 5. (Color online) (a) Stability properties of three multi-pass resonator designs having same eigen-mode waist  $w$ , 16 reflections (per round-trip) at the active medium and a gain medium with a Gaussian aperture of  $W = 20$  mm. The black dotted curve (1 segment containing two passes) represents the stability plot of the single-segment resonator of Fig. 2 (b). It serves as reference. The green curve (8 segments, each containing 2 passes) represents our design as a succession of nearly-identical segments as given in Fig. 2 (d). The fluctuations arise from a small segment-to-segment asymmetry: the distance disk to convex mirror in the first segment has been assumed to be 1518 mm i.e., 20 mm longer than in the other segments. Besides these fluctuations, the stability plot of the multi-segment resonator is identical to the stability plot of the single-segment resonator. The red curve (1 segment containing 16 passes) represents the stability plot for a 4f-based multi-pass resonator. Its stability region is 8 times smaller than the reference because it shrinks with the number of passes. The blue curve (2 segments, each containing 8 passes) represents a merged resonator concept (see Sec. 4) having two segments containing 4f-imaging stages. (b) Corresponding average (over a round-trip) transmission through the Gaussian aperture at the thin-disk for variations of the thin-disk thermal lens.

which does not occur in reality. The inclusion of these soft apertures into the simulations suppresses these gaps as shown in Fig. 4 (e) for the particular case of a two-segment resonator and leaves residual small fluctuations of the eigen-mode waist. Hence, it is essential to compute the stability properties of the multi-pass resonator including soft aperture effects. However, it is important to stress that the general behavior of the stability regions does not critically depend on the exact value of the assumed aperture waist  $W$  as can be deduced by comparing the green with the red curves of Fig. 4 (e).

Also the aperture-related losses per pass (averaged over a round-trip) confirm that when including soft-aperture effects the multi-segment resonator with small asymmetries behaves similar to the single-segment resonator. The residual waist fluctuations arising from the suppression of the gap give rise to a negligible increase of losses per pass compared with the single-segment case as visible by comparing Fig. 4 (f) with Fig. 4 (c).

This behavior can be generalized to many segments: the stability region, mode waist and losses per pass (averaged over a round-trip) for the 8-segment multi-pass resonator of Fig. 2 (d) with small segment-to-segment deviations turn out to be practically identical with the stability region, the mode waist and losses per pass of the underlying segment as demonstrated in Fig. 5 (compare green solid with dashed black curves). The same figure for comparison also shows the smaller stability range featured by the multi-pass resonator based on 4f-imaging stages having the same number of passes and beam size at the active medium.

In summary, the soft aperture effects occurring naturally in the pumped active medium grant the realization of a multi-pass oscillator as a concatenation of several nearly-identical optical



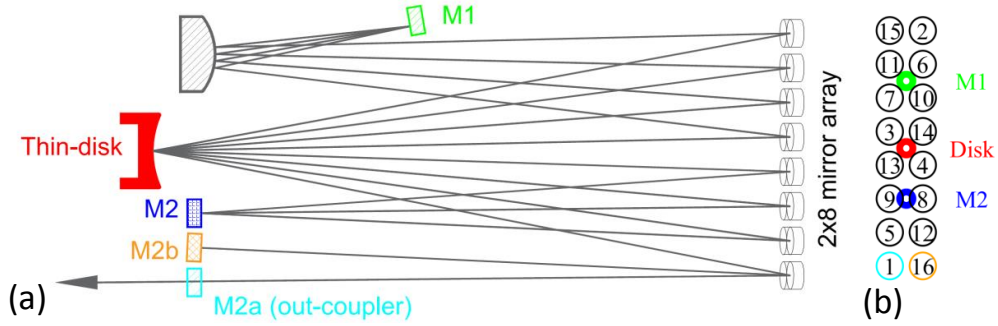


Fig. 6. (Color online) (a) Possible realization of a multi-pass oscillator with 16 reflections at the thin-disk per round-trip achieved by concatenating 8 identical segments. The beam routing requires a mirror-array of 16 flat mirrors which can be individually adjusted. One of the two end-mirrors M2a and M2b could be used as an out-coupler. (b) Mirror-array working principle. The beam routing at the mirror-array plane follows the given numbering and is achieved by successive reflections at the thin-disk, mirror M1 and mirror(s) M2. The projection of these elements are indicated.

segments. When considering aperture effects, the stability region and losses per pass of our multi-segment resonator is practically identical to the stability region of the single-segment resonator. Therefore contrarily to the 4f-based multi-pass resonator, the stability region of our multi-pass resonator does not shrink with the number of passes.

### 3. Proof of principle

For a proof of principle we transformed the multi-pass amplifier [34, 35] that we developed for spectroscopy of muonic atoms [36, 37] into a multi-pass oscillator by adding two end-mirrors. This design schematically depicted in Fig. 6 fulfills our requirements of sufficiently small segment-to-segment variations as it uses the same thin-disk and the same convex mirror in all segments. Moreover the mirror array that is used to fold the beam providing several passes on the same thin-disk also guarantees similar path lengths and small incident angles.

The beam routing in this multi-pass oscillator obeys the following scheme. Starting from the out-coupler M2a the beam is reflected at the array-mirror 1 towards the thin-disk. From here, it proceeds towards the array-mirror 2 and the convex mirror until it reaches M1. From M1 the beam travels back to the array at array-mirror 3, then to the thin-disk and the array-mirror 4 until it reaches the mirror M2. This scheme is iterated until the beam passes the array-mirror 16 and is back-reflected at the second end-mirror M2b. From here the beam propagates the same path backwards until it reaches again mirror M2a closing the round-trip. The beam routing at the mirror-array position given by the numbering as shown in Fig. 6 (b) can be thus understood as alternating point-reflections at the thin-disk, M1 and M2 mirrors projections.

The multi-pass oscillator (with 16 reflections at the thin-disk per round-trip) whose underlying segment specifications are given in Fig. 2 (a) has been tested in cw mode using a flat out-coupler with 50% transmission. As active medium, a 345  $\mu\text{m}$  thick Yb:YAG thin-disk with 5% nominal doping concentration contacted by TRUMPF to a water-cooled CVD-diamond heat sink having a 4 m radius of curvature has been used. Even though the choice of the thin-disk parameters were optimized for low repetition rate Q-switched operation, encouraging output powers and slope efficiency (40% in fundamental mode operation) have been observed as shown in Fig. 7. This represents the first preliminary demonstration of the applicability of our multi-pass oscillator concept, in particular showing that the soft aperture effects naturally present in the

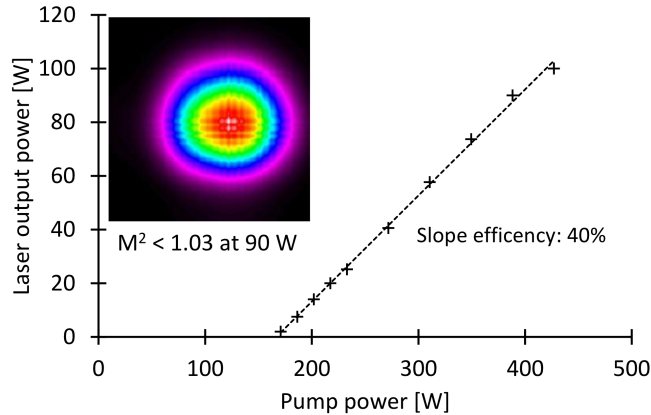


Fig. 7. (Color online) Input-output characteristics of the multi-pass resonator based on our design with 16 reflections per round-trip. The measurements have been accomplished in a cw operation for a Yb:YAG thin-disk of  $345 \mu\text{m}$  thickness, a  $940 \text{ nm}$  pump wavelength and an out-coupling mirror reflectivity of 50%. The inset shows the measured output beam.

pumped active medium are sufficient to suppress the instabilities related to the various segment-to-segment asymmetries associated with the practical realization of a multi-pass scheme.

#### 4. A simple way to improve the multi-pass resonator based on 4f imaging

The multi-pass oscillators based on 4f-imaging stages show an enhanced sensitivity to thermal lens effects as illustrated by the shrinking of the stability region with the number of passes in Fig. 1. However, a major advantage of the 4f-scheme is that a sequence of several 4f-imaging stages can be realized using only few optical elements as shown in Fig. 8 (a) whose working principle is detailed in [38, 39, 40]. On the other hand, our multi-pass oscillator concept has a superior stability for variations of the thermal lens, but it requires an array of mirrors resulting in increased mechanical complexity.

In Fig. 8 (b) we present an optical layout which results from merging the two concepts. It consists of a concatenation of two optically stable segments (according to our scheme) each containing a multi-pass sequence based on 4f-imaging stages. As this merging can be achieved by a simple rearrangement of the optics used in the 4f-based system, it inherits a similar beam waist evolution (see Fig. 8 (b) and (d)) and its simplicity, qualifying this scheme for industrial applications. At the same time this merged layout shows improved stability because the stability region of our concept does not shrink with the number of segments. The resulting stability region of this merged scheme (two segments, each containing  $N/2$  4f-propagations) is a factor of two larger compared to the standard 4f-schemes (one segment with  $N$  4f-propagations) as visible from the comparison of the blue and red curves in Fig. 5, provided both multi-pass resonators have the same number of passes. Thus, with a simple rearrangement of the beam path structure of the standard 4f-design (but using the same optical elements) a factor of two larger stability region can be obtained opening the way to larger pump power density, beam waists and number of passes.

#### 5. Conclusions

We have presented a multi-pass resonator scheme as a sequence of nearly-identical optically stable segments, each segment containing the same active medium featuring soft-aperture effects. The stability region of such a multi-segment resonator does not decrease with the number

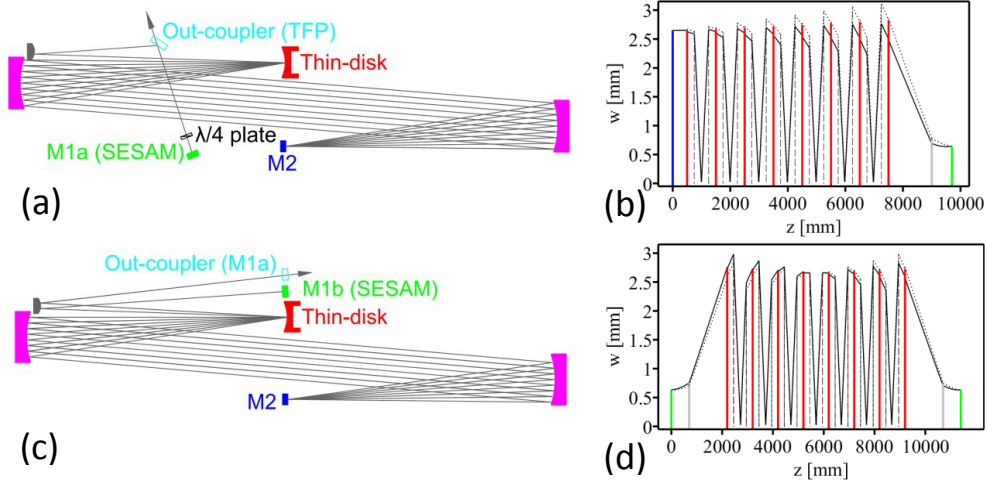


Fig. 8. (Color online) (a) Multi-pass oscillator based on 4f-imaging stages. Multiple 4f-imaging stages can be implemented using the same optical elements which simplifies the mechanical realization and decreases the production costs. TFP: thin-film polarizer. (b) Corresponding eigen-mode waist evolution. Due to soft aperture effects the back (dotted line) and forth (continuous line) propagations have different waists. The vertical red lines represent the position of the thin-disk. (c) Schematic of the merged concept with two segments, each containing half the number of reflections on the thin-disk as in (a). (d) Corresponding eigen-mode waist evolution.

of segments. Therefore this concept solves the limitations of state-of-the-art multi-pass resonators based on 4f-imaging stages which feature a shrinking of the stability region with the number of passes on the active medium.

We have demonstrated that it is essential to include the soft aperture effects occurring in the active medium into the simulations. They suppress the formation of gaps within the stability region which would arise as a consequence of small segment-to-segment asymmetries associated with the practical realization of a multi-pass system. This has been achieved by implementing effective Gaussian apertures into the ABCD-matrix formalism as lenses with imaginary focal length.

The multi-pass resonator concept presented here requires small segment-to-segment asymmetries achievable using the same active medium in all passes. Larger segment-to-segment deviations would cause increased losses (decreased transmission through the aperture) which strongly reduce laser efficiency or even disrupt laser operation.

This multi-pass resonator layout is particularly suited for ultrafast lasers where the mode-locking mechanism is based on SESAM technologies [12]. The SESAM could be placed at the position of one of the resonator end-mirrors (e.g. mirror M2b in Fig. 6) as at this position there is minimal intracavity intensity and the SESAM mirror would be intersected only once per round-trip. This scheme having several passes on the active medium and large cavity lengths paves the way for energy and power scaling of mode-locked lasers expanding greatly the range of applications for ultrashort pulses delivered directly by a laser oscillator.

## 6. Acknowledgments

We would like to thank R. Pohl and F. Kottmann. We acknowledge the support from the Swiss National Science Foundation: Projects SNF\_200020\_159755 and SNF\_200021\_165854.